Nano Vision, Vol.2 (1,2&3), 25-47 (2012)

Stannum-Cadmium Composite Nano Rods Nano Wires and Particles by Simple Technique

S. SAKTHIVEL[1], S. RAJIVGANDHI[1] and D. MANGALARAJ[2]

[1]Thinfilm Physics and Nano Science Laboratory,
PG and Research Department of Physics,
Rajah Serfoji Govt. College, Thanjavur -613 005, Tamilnadu, INDIA.
[2]Department of Nano Science and Nano Technology,
Bharathiar University, Coimbatore- 641 046, Tamilnadu, INDIA.

(Received on: April 4, 2012)

ABSTRACT

Stannum - Cadmium (Sn-Cd) composite nano rod (nr), nano wires (nw) and nano particles (np) were synthesized at a stretch using new chemical technique. The temperature required for fabricating nr, nw and np is 383 K. X – ray diffraction (XRD) peaks indicates the diffraction of x-ray nr, np and nw. Exactly fifty six peaks were found and these are the combination of Sn-Cd nano composites. The average size of the nano rods is 52.69 nm and the rods size ranging from 32.90 nm to 68.70 nm. The d-spacing value of the nano rods varying from 7.6884 Å to 1.2125Å. Dislocation density values changing from $2.11 – 9.23 \times 10^{14}$ m^{-2}.

Keywords: Sn-Cd, Tin , Cadmium, nano rods, nano wires and nano particles.

1. INTRODUCTION

Nanowires, nanorods and nanotubes play a very important role in nanoelectronics Patently M. J., 2004; Bharat Bhushan,2004; Yang P. *et al.*, 2002. They have many applications in many fields such as for making nanowires connecting between nano devices in modern nanoelectronic circuits, for tips or probes in modern microscopes, for making various kinds of sensors and pn junction diodes, swishings, memory nodes, nanowire FET devices Lauhon L. J. *et al*., 2004; Huang Y. *et al*., 2002; Greytak A. B. *et al*., 2004; Atashbar M Z *et al*., 2002. The nano structures of the nanorods plays an important role as building blocks in devices and processes, such as light emitting diodes, solar cells, single electron transistors, lasers, and biological labels Agarwal, R. *et al*.,

2005; Hu, J. *et al*., 2001; Friedman, R. S. *et al*., 2005; Hong, B. H. *et al*., 2001; Huynh, W. U, *et al*., 2002.

In nanotechnology, nano rods are one morphology of nanoscale objects. Each of their dimensions range from 1–100 nm. They may be synthesized from metals or semi-conducting materials. In 2006, Ramanathan *et al*. demonstrated Ramanathan S. *et al*., 2006 electric-field mediated tunable photoluminescence from ZnO nanorods, with potential for application as novel sources of near-ultraviolet radiation.

Unidirectional nano rods, wires, tubes, ribbons and belts nano structures have attracted considerable attention. The nano structures represents various physical properties like optical, electrical and mechanical properties.

Many modern methods based on physical and chemical approaches have been developed for the synthesis of controlled size and shape of one-dimensional nanostructures, including, for example, vapor-liquid-solid and the solution liquid-solid processes, solvothermal, template-assisted, kinetic growth control, self-assembly, and thermolysis of a single-source precursor in ligating solvents Nedeljkovic, J.M. *et al*.,2004; Kan,S. *et al*., 2003; Tang.Z *et al*., 2002; Panda, A. B. et al.,2005; Nikoobakht, B. *et al*., 2000; Yin, M. *et al*., 2004; Barrelet,C.J. *et al*., 2003; Manna, L. *et al*., 2000; Pradhan, N. *et al*., 2004; Lu, Q. *et al*.,2004; Liu,X *et al*.,2004 ; Peng, X. *et al*., 2000 ; Li,Y. *et al*., 2004.

The VLS mechanism circumvents this by introducing a catalytic liquid alloy phase which can rapidly adsorb a vapor to supersaturation levels, and from which crystal growth can subsequently occur from nucleated seeds at the liquid-solid interface.

Using the solvothermal route gains one the benefits of both the sol-gel Oliveira, Marcela M. *et al*., 2003 and hydrothermal routes Andersson, Martin *et al*.,2002. Thus solvothermal synthesis allows for the precise control over the size, shape distribution, and crystallinity of metaloxide nanoparticles or nanostructures.

Self-assembly (SA) in the classic sense can be defined as the spontaneous and reversible organization of molecular units into ordered structures by non-covalent interactions. The first property of a self-assembled system that this definition suggests is the spontaneity of the self-assembly process: the interactions responsible for the formation of the self-assembled system act on a strictly local level in other words, the nanostructure builds itself.

In the recent years various semi-conducting nanorods are fabricated by various methods Anukorn Phuruangrat *et al*., 2009; Quang Trung Khuc *et al*., 2010; Asit Baran Panda *et al*., 2006.

But no work so far published on semi-conducting alloys. We sure that on work totally new for alloy nanorods research field. Present work deals with equal percentage of semi-conducting alloys for fabrication of nanorods / nano particles. So many important observation were obtained and presented in this paper.

Eventhough lot of work carried out on Cadmium and Tin seperately, it is very limited work on Sn-Cd composite and alloy nano rods , nano wires and nano particles.

2. EXPERIMENTS

Initially 68 gram Cadmium chloride was dissolved by 50 millilitre distilled water and 42 gram tin chloride was dissolved by 50 millilitre distilled water and stirred well by using magnetic stirrer for 1 hour.

Bulk Cadmium chloride material of purify 99.9% were taken and dissolved by distilled water. After that the solution containing Cadmium particles were stirred for 1 hour. Finally a complete transparent solution containing nano particles were used for preparing nano Cadmium rods by various techniques like drop,rollilg …etc. Similarly Tin nano particles were fabricated. These two solutions are properly mixed in the ratio of 10:30 ml of $CdCl_2$: $SnCl_2$ respectively by using magnetic stirrer for half an hour.

A well cleaned cylindrical glass rod were immersed in a beaker containing transparent Cadmium chloride-Tin chloride solution. The immersed rod was rolled over a well ultrasonically cleaned glass substrate. After taking the glass plate , it was kept in the open atmosphere for two to three hours. Finally the required nanorods were fabricated and apply for various studies. The coated glass plate has only tin particles on the Cadmium nanorods and it was continued by XRD and SEM. The different stages of rolling methods are shown in the figure 2.1(a-d).

Dip coating is a popular way of creating thin films for research purposes. Uniform films can be applied onto flat or cylindrical substrates.

The following five stages involved in the dip coating process Rahaman, M.N..,2007:

Immersion

The substrate is immersed in the solution of the coating material at a constant speed (preferably jitter-free).

Start-up

The substrate has remained inside the solution for a while and is starting to be pulled up.

Deposition

The thin layer deposits itself on the substrate while it is pulled up. The withdrawing is carried out at a constant speed to avoid any jitters. The speed determines the thickness of the coating (faster withdrawal gives thicker coating material).

Drainage

Excess liquid will drain from the surface.

Evaporation

The solvent evaporates from the liquid, forming the thin layer. For volatile solvents, such as alcohols, evaporation starts already during the deposition & drainage steps.

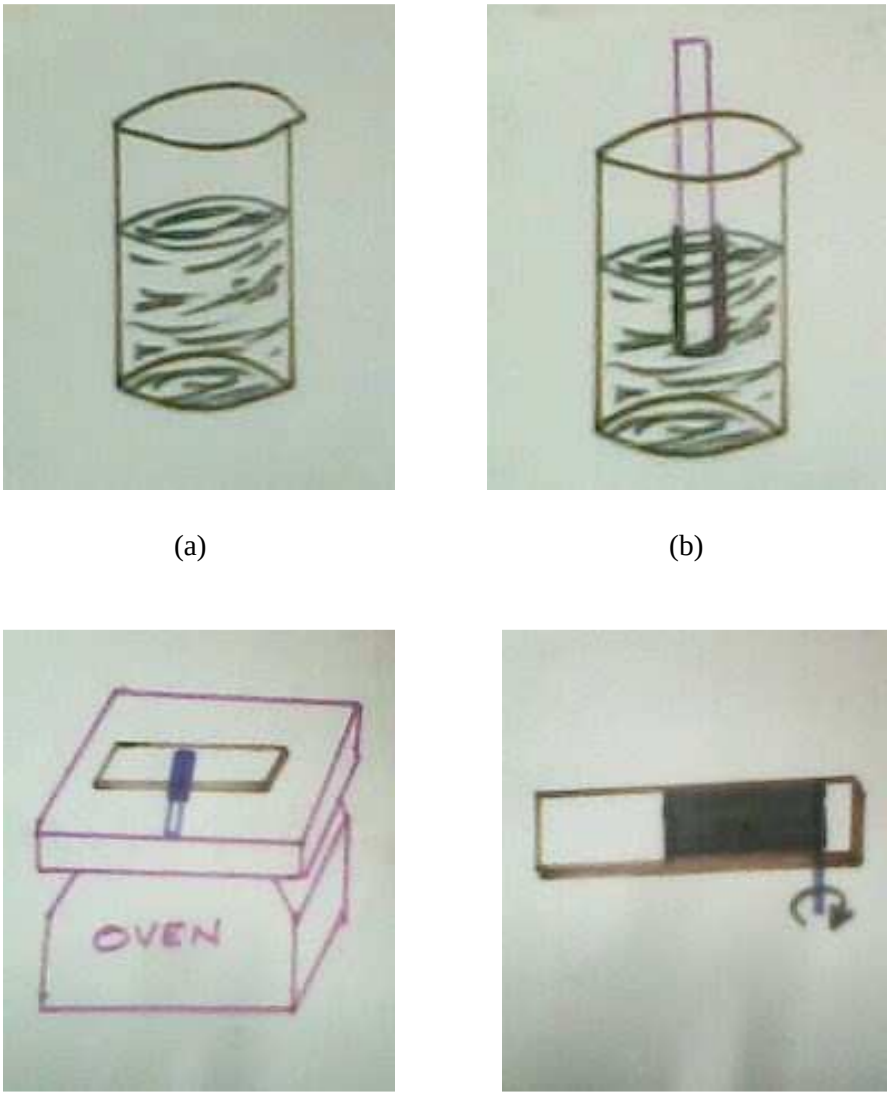

(a) (b)

(c) (d)

Figure 2.1(a-d) Block diagrams of Rolling Method

a. Sn-Cd composite solution
b. Glass rod immersed in the solution
c. Start up rolling
d. Sn-Cd composite sample

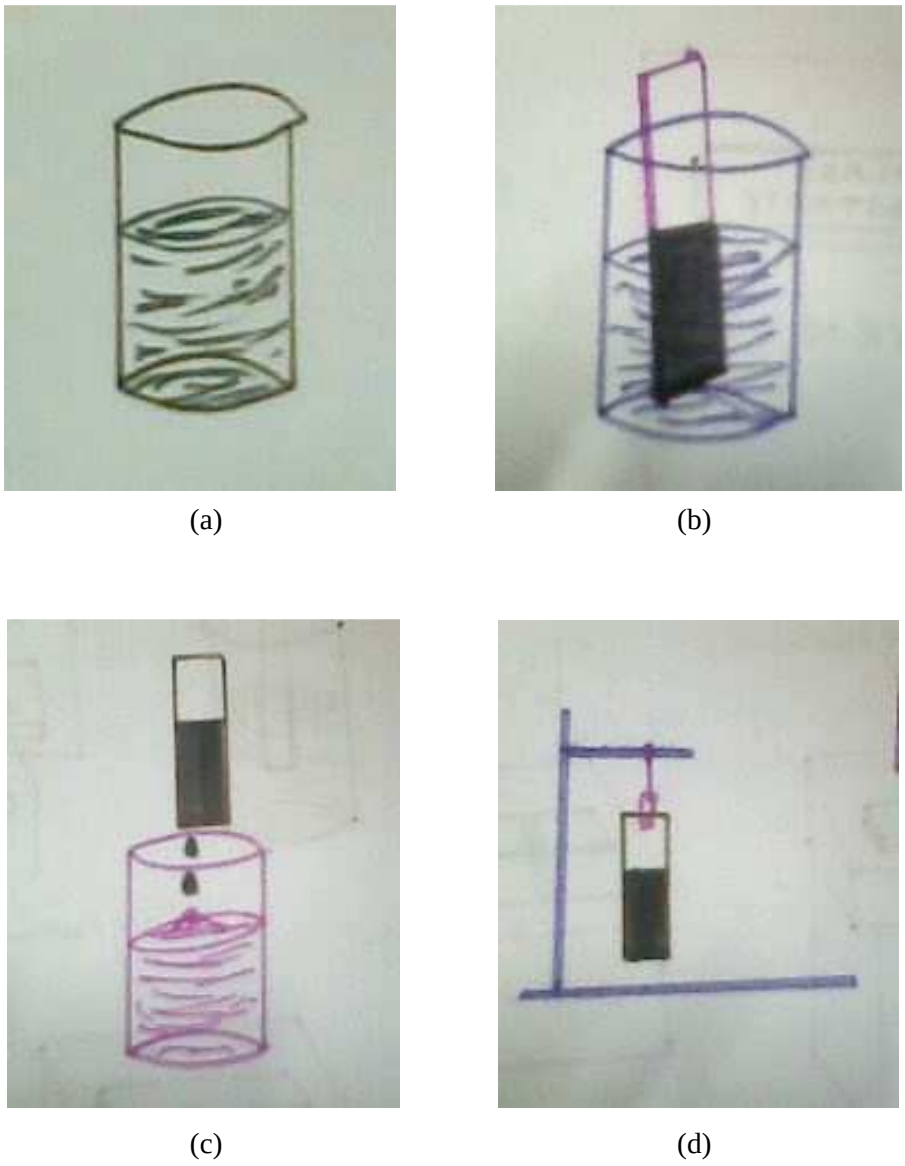

(a) (b)

(c) (d)

Figure 2.2. Block diagrams of Dip coating Method

a. Sn-Cd composite solution
b. Glass substrate immersed in the solution
c. Take the substrate from the solution
d. Sn-Cd composite sample drying at open atmosphere

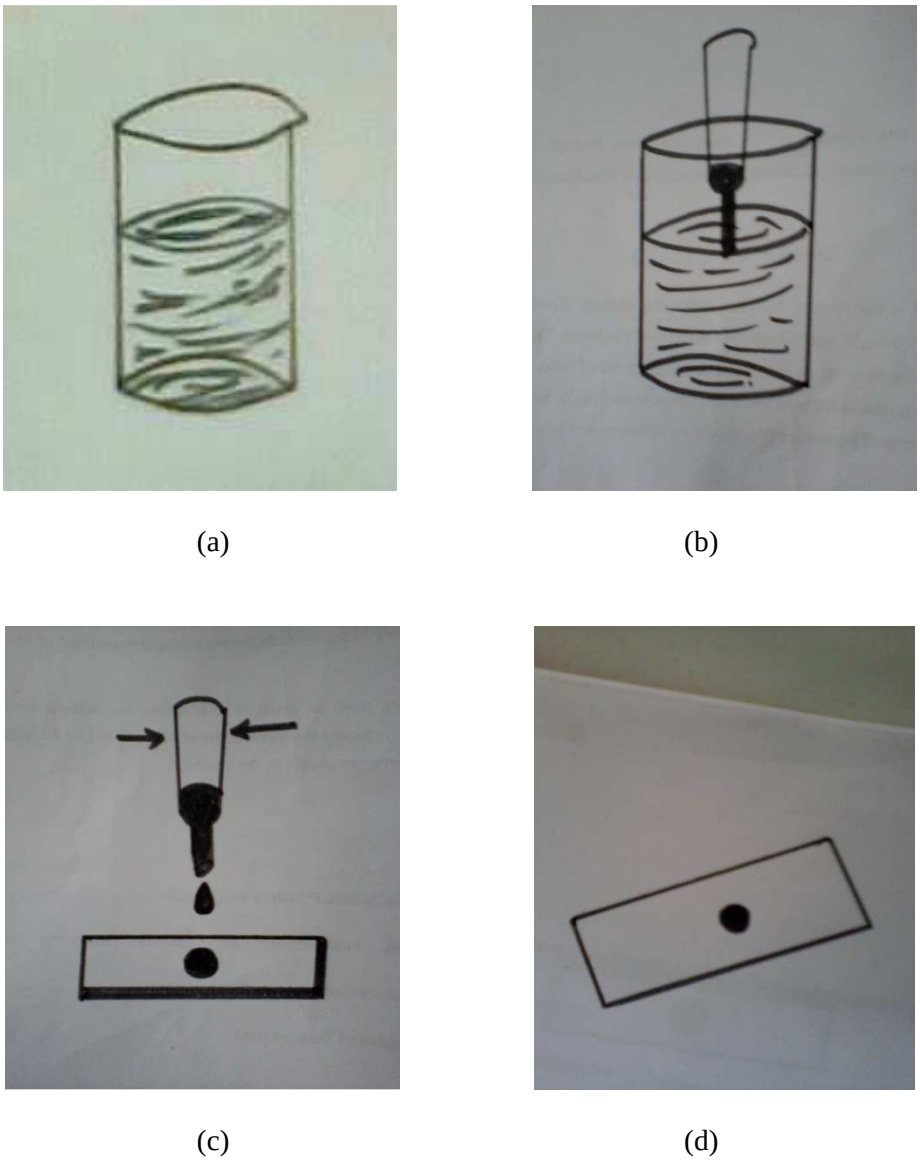

(a) (b)

(c) (d)

Figure 2.3. Block diagrams of Drop Method

a. Sn-Cd composite solution
b. Filler inserted in the solution
c. Press the filler for drop on the well cleaned substrate
d. Sn-Cd composite sample drying at open atmosphere

In the continuous process, the steps are carried out directly after each other. The various stages of dip coating process are shown in the figure 2.2 (a-d).

A Ultrasonically cleaned cylindrical glass rod were immersed in a beaker containing transparent Cadmium chloride-Tin chloride solution. The immersed rod was dropped over an ultrasonically cleaned glass substrate. After pull out the glass plate, it was kept in the open atmosphere for two to three hours. Finally the required nanorods were fabricated and apply for various studies. The coated glass plate has only tin particles on the cadmium nanorods and it was continued by XRD and SEM. The different stages of rolling methods are shown in the figure 2.3(a-d).

The vapor-liquid-solid method (VLS) is a mechanism for the growth of one-dimensional structures, such as nanowires, from chemical vapor deposition. Growth of a crystal through direct adsorption of a gas phase on to a solid surface is generally very slow. Sn-Cd composite nanorods and/or particles were grownd and it was taken for further studies. Lu, Yicheng *et al*.,2004.

2.1 X-ray diffraction techniques

Crystals are regular arrays of atoms, and X-rays can be considered waves of electromagnetic radiation. Atoms scatter X-ray waves, primarily through the atoms' electrons. Just as an ocean wave striking a lighthouse produces secondary circular waves emanating from the lighthouse, so an X-ray striking an electron produces secondary spherical waves emanating from the electron. This phenomenon is known as elastic scattering, and the electron (or lighthouse) is known as the scatterer.

A regular array of scatterers produces a regular array of spherical waves. Although these waves cancel one another out in most directions through destructive interference, they add constructively in a few specific directions, determined by Bragg's law:

$$2d\sin\theta = n\lambda \qquad (2.1)$$

Here ‘d’ is the spacing between diffracting planes, ‘θ’ is the incident angle, ‘n’ is any integer, and’λ’ is the wavelength of the beam. These specific directions appear as spots on the diffraction pattern called reflections. Thus, X-ray diffraction results from an electromagnetic wave (the X-ray) impinging on a regular array of scatterers (the repeating arrangement of atoms within the crystal).

X-rays are used to produce the diffraction pattern because their wavelength λ is typically the same order of magnitude (1-100 Ångströms) as the spacing d between planes in the crystal.

2.2 Scanning Electron Microscope (SEM)

A scanning electron microscope (SEM) is a type of electron microscope that images a sample by scanning it with a high-energy beam of electrons in a raster scan pattern. The electrons interact with the atoms that make up the sample producing signals that contain information about the sample's surface topography, composition, and other properties such as electrical conductivity.

In a typical SEM, an electron beam is thermionically emitted from an electron gun fitted with a tungsten filament cathode.

Tungsten is normally used in thermionic electron guns because it has the highest melting point and lowest vapour pressure of all metals, thereby allowing it to be heated for electron emission, and because of its low cost. Other types of electron emitters include lanthanum hexaboride (LaB_6) cathodes, which can be used in a standard tungsten filament SEM if the vacuum system is upgraded and field emission guns (FEG), which may be of the cold-cathode type using tungsten single crystal emitters or the thermally-assisted Schottky type, using emitters of zirconium oxide.

The electron beam, which typically has an energy ranging from 0.5 to 40 keV, is focused by one or two condenser lenses to a spot about 0.4 to 5 nm in diameter. The beam passes through pairs of scanning coils or pairs of deflector plates in the electron column, typically in the final lens, which deflect the beam in the x and y axesso that it scans in a raster fashion over a rectangular area of the sample surface.

When the primary electron beam interacts with the sample, the electrons lose energy by repeated random scattering and absorption within a teardrop-shaped volume of the specimen known as the interaction volume, which extends from less than 100 nm to around 5 µm into the surface. The size of the interaction volume depends on the electron's landing energy, the atomic number of the specimen and the specimen's density. The energy exchange between the electron beam and the sample results in the reflection of high-energy electrons by elastic scattering, emission of secondary electrons by inelastic scattering and the emission of electromagnetic radiation, each of which can be detected by specialized detectors.

The beam current absorbed by the specimen can also be detected and used to create images of the distribution of specimen current. Electronic amplifiers of various types are used to amplify the signals which are displayed as variations in brightness on a cathode ray tube. The raster scanning of the CRT display is synchronised with that of the beam on the specimen in the microscope, and the resulting image is therefore a distribution map of the intensity of the signal being emitted from the scanned area of the specimen.

The image may be captured by photography from a high resolution cathode ray tube, but in modern machines is digitally captured and displayed on a computer monitor and saved to a computer's hard disk.

2.3 UV-Visible Spectrometer

Ultraviolet-visible spectroscopy or ultraviolet-visible spectrophotometry (UV-Vis or UV/Vis) refers to absorption spectroscopy or reflectance spectroscopy in the ultraviolet-visible spectral region. This means it uses light in the visible and adjacent (near-UV and near-infrared (NIR)) ranges. The absorption or reflectance in the visible range directly affects the perceived color of the chemicals involved. In this region of the electromagnetic spectrum, molecules undergo electronic transitions. This technique is complementary to fluorescence spectroscopy, in that fluorescence deals with transitions from the excited state to the ground state, while absorption measures transitions from the ground state to the excited state.

The basic parts of a spectrophotometer are a light source, a holder for the sample, a diffraction grating in a

monochromator or a prism to separate the different wavelengths of light, and a detector. The radiation source is often a Tungsten filament (300-2500 nm), a deuterium arc lamp, which is continuous over the ultraviolet region (190-400 nm), Xenon arc lamps, which is continuous from 160-2,000 nm; or more recently, light emitting diodes (LED) for the visible wavelengths. The detector is typically a photomultiplier tube, a photodiode, a photodiode array or a charge-coupled device(CCD). Single photodiode detectors and photomultiplier tubes are used with scanning monochromators, which filter the light so that only light of a single wavelength reaches the detector at one time. The scanning monochromator moves the diffraction grating to "step-through" each wavelength so that its intensity may be measured as a function of wavelength. Fixed monochromators are used with CCDs and photodiode arrays. As both of these devices consist of many detectors grouped into one or two dimensional arrays, they are able to collect light of different wavelengths on different pixels or groups of pixels simultaneously.

A spectrophotometer can be either single beam or double beam. In a single beam instrument (such as the Spectronic 20), all of the light passes through the sample cell. I_o must be measured by removing the sample. This was the earliest design, but is still in common use in both teaching and industrial labs.

In a double-beam instrument, the light is split into two beams before it reaches the sample. One beam is used as the reference; the other beam passes through the sample. The reference beam intensity is taken as 100% Transmission (or 0 Absorbance), and the measurement displayed is the ratio of the two beam intensities. Some double-beam instruments have two detectors (photodiodes), and the sample and reference beam are measured at the same time. In other instruments, the two beams pass through a beam chopper, which blocks one beam at a time. The detector alternates between measuring the sample beam and the reference beam in synchronism with the chopper. There may also be one or more dark intervals in the chopper cycle. In this case the measured beam intensities may be corrected by subtracting the intensity measured in the dark interval before the ratio is taken.

Samples for UV/Vis spectrophotometry are most often liquids, although the absorbance of gases and even of solids can also be measured. Samples are typically placed in a transparent cell, known as a cuvette. Cuvettes are typically rectangular in shape, commonly with an internal width of 1 cm. Test tubes can also be used as cuvettes in some instruments. The type of sample container used must allow radiation to pass over the spectral region of interest. The most widely applicable cuvettes are made of high quality fused silica or quartz glass because these are transparent throughout the UV, visible and near infrared regions. Glass and plastic cuvettes are also common, although glass and most plastics absorb in the UV, which limits their usefulness to visible wavelengths.

Specialized instruments have also been made. These include attaching spectrophotometers to telescopes to measure the spectra of astronomical features. UV-visible micro spectrophotometers consist of

a UV-visible microscope integrated with a UV-visible spectrophotometer.

A complete spectrum of the absorption at all wavelengths of interest can often be produced directly by a more sophisticated spectrophotometer. In simpler instruments the absorption is determined one wavelength at a time and then compiled into a spectrum by the operator. By removing the concentration dependence, the extinction coefficient (ε) can be determined as a function of wavelength.

It measures the intensity of light passing through a sample (I), and compares it to the intensity of light before it passes through the sample (I_o). The ratio I / I_o is called the transmittance, and is usually expressed as a percentage (%T). The absorbance, A, is based on the transmittance:

$$A = -\log(\%T / 100\%) \quad (2.2)$$

The UV-visible spectrophotometer can also be configured to measure reflectance. In this case, the spectrophotometer measures the intensity of light reflected from a sample (I), and compares it to the intensity of light reflected from a reference material (I_o)(such as a white tile). The ratio I / I_o is called the reflectance, and is usually expressed as a percentage (%R).

3. RESULT AND DISCUSSION

X-ray diffraction patterns of nanorods and nano particles prepared by using simple techniques are presented in figure 3.1. The obtained peaks in the diffraction spectra indicates the polycrystalline nature of the nano structures. The peak positions are well matched with Cd X-ray pattern [S. Sakthivel *et al*.,2011] other than Sn-Cd composite nano rods /particles, no other by productsare found in the pattern [S. Sakthivel *et al*.,2011] . This indicates that the purity of the Sn-Cd composite nanorods / nano particles . If we go further with high temperature and time treatment there is a possibility or getting good crystallinity. From this finding it is important that the hydrothermal treatment temperature and time are very important to get pure phase of Sn-Cd composite with required important crystallinity.

The d spacing value of the nano crystal varying from 7.688 Å to 1.212 Å[Annamalai *et al*., 2010] calculated the lattice parameter of the hydrothermally synthesized Sn-Cd composite nanorods / nano particles as 8.62 Å using multiple XRD peaks and least-squares method, which is with in the range of previously reported values [Zeng J. *et al.*, 2008]. No peaks originating from impurities could be seen indicating the formation of pure Sn-Cd composite nanorods / nano particles. The average particle size calculated from the X-ray diffraction for the as prepared Sn-Cd composite particles was 52.69 nm and ranging from 32.90 nm to 68.70 nm more than 56 peaks were observed due to the contribution of Sn-Cd composite nanorods / nano particles in figure 3.2. The 2θ, flex width, d- spacing intensity and I/I_0 value of the X-ray were displayed in table 3.1.

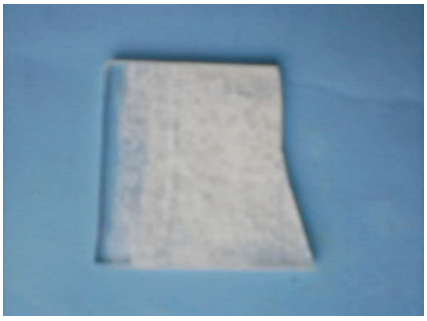

Figure 3.1. Sn-Cd composite nr,nw and np

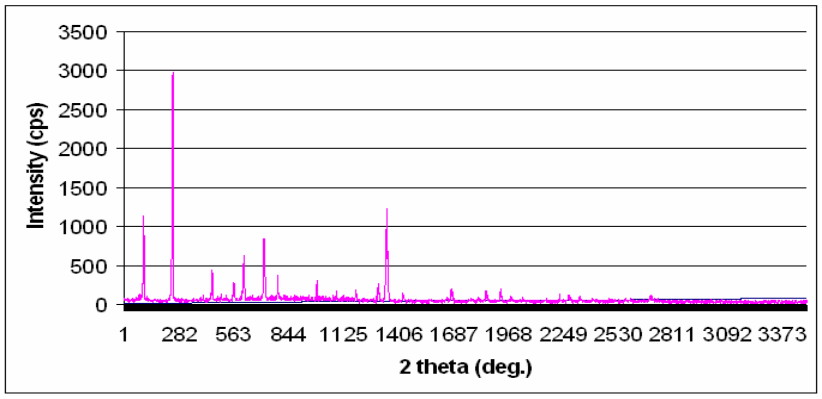

Figure 3.2. XRD Pattern of Sn-Cd composite nano rods/ particles.

Table 3.1 XRD peak search value of Sn – Cd composite Nanorods / Nano particles

Peak Search

Sample	: sr1	File	: tsr1.raw	Date	: May-31-11 18:50:11	Operator	: rigaku
Comment	:	Memo	:				
Method	: 2nd differential	Typical width	: 0.250 deg.	Min. height	: 18.00 cps		

Peak no.	2theta	Flex	Width	d-value	Intensity	I/Io	Peak no.	2theta	Flex	Width	d-value	Intensity	I/Io
1	11.500		0.165	7.6884	130	5	31	43.020		0.138	2.1038	90	3
2	11.980		0.141	7.3814	850	31	32	43.520		0.165	2.0778	197	7
3	14.920		0.165	5.9328	2900	100	33	46.240		0.138	1.9617	77	3
4	18.960		0.165	4.6719	387	14	34	47.040		0.141	1.9302	160	6
5	19.960		0.165	4.4447	103	4	35	48.520		0.141	1.8747	187	7
6	20.440		0.141	4.3414	90	4	36	49.660		0.141	1.8364	83	3
7	21.260		0.165	4.1757	263	10	37	50.360		0.141	1.7938	80	3
8	22.220		0.165	3.9974	603	21	38	51.440		0.141	1.7749	43	2
9	22.640		0.141	3.9242	87	3	39	52.260		0.141	1.7490	53	2
10	22.860		0.165	3.8870	87	3	40	53.760		0.141	1.7037	60	3
11	23.080		0.141	3.8504	85	3	41	54.600		0.141	1.6795	153	5
12	24.300		0.141	3.6598	843	30	42	55.520		0.141	1.6538	100	4
13	25.740		0.165	3.4582	343	12	43	56.680		0.138	1.6227	87	3
14	26.300		0.141	3.3858	100	4	44	57.500		0.165	1.5913	60	3
15	28.880		0.165	3.0890	57	2	45	60.260		0.165	1.5348	40	2
16	29.720		0.188	3.0035	303	11	46	61.920		0.165	1.4973	80	3
17	30.240		0.165	2.9531	97	4	47	64.020		0.141	1.4532	70	3
18	31.720		0.165	2.8186	157	6	48	64.520		0.165	1.4431	53	2
19	32.020		0.141	2.7878	77	3	49	65.480		0.141	1.4245	37	2
20	32.560		0.141	2.7477	77	3	50	67.080		0.212	1.3932	47	2
21	33.720		0.165	2.6558	177	7	51	70.340		0.141	1.3373	37	2
22	34.760		0.188	2.5787	57	2	52	71.160		0.165	1.3239	67	3
23	35.200		0.141	2.5475	67	3	53	75.020		0.141	1.2659	37	2
24	36.040		0.165	2.4900	267	10	54	75.960		0.165	1.2517	50	2
25	36.880		0.165	2.4352	1230	43	55	78.680		0.141	1.2151	40	2
26	38.580		0.235	2.3317	143	5	56	78.880		0.141	1.2125	47	2
27	39.400		0.141	2.2851	97	3							
28	40.180		0.141	2.2446	47	2							
29	41.140		0.141	2.1923	70	3							
30	42.560		0.165	2.1224	67	3							

June-03-2011 15:53:26 Page-2

The d spacing value and full wave at half maximum(FWHM) for each crystalline size were given in the table 3.2. Crystalline size of the nanorods / nano particles were calculated using Debye-Sherrer formula,

$$D = k\lambda / \beta\cos\theta \quad (3.1)$$

Where,

K is the particle shape factor (0.827),

λ is the wavelength of the X-ray used,

β is the calibrated half intensity width of the selected diffraction peak,

θ is the Bragg's angle.

Using the above formula, we calculated the average grain size is 52.69 nm.

UV- Visible Spectroscopy was used to characterize the optical absorptions of Sn-Cd composite nanorods / nano particles. It is well known that theory of optical absorption gives the relationship between the absorption coefficients 'α' and photon energy 'hν' for direct allowed transition as

$$(\alpha h\nu)^2 = B (h\nu - E_g) \quad (3.2)$$

Where,

hν is the photon energy,

E_g is the apparent optical band gap,

B is the semiconductor characteristic constant,

α is the absorption coefficient.

Sn-Cd composite nr,nw & np are calculate using 'C' program. The program used for calculating grain size and band gap energy are presented given below

Determination of grain size 'D' using C program:

Formula :

$$D = \kappa \lambda / \beta\cos\theta$$

Program :

```
#include<stdio.h>
#include<conio.h>
#include<math.h>
void main()
{
float k=0.827;
float lam=1.524;
float d,beta,theta;
clrscr();
printf("Enter the Beta and Theta value :\n\n");
scanf("%f%f",&beta,&theta);
d=((k*lam)/beta*cos(theta));
printf("The Grain Size =%f x10^(-10)",d);
getch();
}
```

Calculation of Band gap energy (Eg) using C program:

Formula:

$$(\alpha h\nu)^2 = B(h\nu - E_g)$$

Program:

```
#include<stdio.h>
#include<conio.h>
#include<math.h>
void main()
{
 float a=2;
 float h=6.626;
 float v,e;
 clrscr();
 printf("Enter the v value :\n\n");
 scanf("%32f",&v);
 e=(sqrt(a*h*v)/(h*v));
 printf("The Energy Band gap
Value=%fx10^(-20)",e);
 getch();
 }
```

Table 3.2. Grain size of Sn-Cd composite nr,nw & np

	Peak	(θ)	(β)	d(Å)	D δ
1	5.750	0.165	7.6884	45.71	4.78
2	5.990	0.141	7.3814	53.35	3.51
3	7.460	0.165	5.9328	45.87	4.75
4	9.490	0.165	4.6719	46.11	4.70
5	9.960	0.165	4.4447	46.17	4.69
6	10.220	0.141	4.3414	53.91	3.44
7	10.630	0.165	4.1757	46.27	4.67
8	11.110	0.165	3.9974	46.35	4.65
9	11.320	0.141	3.9242	54.11	3.41
10	11.430	0.165	3.8870	46.40	4.64
11	11.540	0.141	3.8504	54.15	3.41
12	12.150	0.141	3.6598	54.27	3.39
13	12.670	0.165	3.4582	46.61	4.60
14	13.150	0.141	3.3858	54.49	3.36
15	14.440	0.165	3.0890	46.96	4.53
16	14.860	0.188	3.0035	41.17	5.89
17	15.120	0.165	2.9531	47.11	4.50
18	15.860	0.165	2.8186	47.28	4.47
19	16.040	0.141	2.7878	55.21	3.28
20	16.280	0.141	2.7477	55.27	3.27
21	16.860	0.165	2.6558	47.52	4.42
22	17.380	0.188	2.5787	41.70	5.75
23	17.600	0.141	2.5475	55.66	3.22
24	18.020	0.165	2.4900	47.82	4.37
25	18.440	0.165	2.4352	47.94	4.35
26	19.290	0.235	2.3317	32.90	9.23
27	19.700	0.141	2.2851	56.36	3.14
28	20.070	0.141	2.2446	56.49	3.13
29	20.570	0.141	2.1923	56.67	3.11
30	21.280	0.165	2.1224	48.81	4.19
31	21.510	0.188	2.1008	42.77	5.46
32	21.760	0.165	2.0778	48.97	4.17
33	23.120	0.188	1.9617	43.27	5.34
34	23.520	0.141	1.9302	57.87	2.98

35	24.260	0.141	1.8747	58.20	2.95
36	24.800	0.141	1.8364	58.45	2.92
37	25.430	0.141	1.7938	58.75	2.89
38	25.720	0.141	1.7749	58.89	2.88
39	26.130	0.141	1.7490	59.10	2.86
40	26.880	0.141	1.7037	59.49	2.82
41	27.300	0.141	1.6795	59.71	2.80
42	27.760	0.141	1.6538	59.96	2.78
43	28.340	0.188	1.6227	45.21	4.89
44	28.950	0.165	1.5913	51.97	3.70
45	30.130	0.165	1.5345	52.58	3.61
46	30.960	0.165	1.4973	53.03	3.55
47	32.010	0.141	1.4532	62.63	2.54
48	32.260	0.165	1.4431	53.78	3.45
49	32.740	0.141	1.4243	63.08	2.51
50	33.840	0.212	1.3832	41.43	5.82
51	35.170	0.141	1.3373	64.89	2.39
52	35.580	0.165	1.3279	55.92	3.19
53	37.510	0.141	1.2650	66.89	2.23
54	37.980	0.165	1.2517	57.70	3.00
55	39.340	0.141	1.2151	68.60	2.12
56	39.440	0.141	1.2125	68.7	2.11

The optical band gap for the absorption edge can therefore be obtained by extrapolating the linear potion of $(\alpha h\nu)^2$ - $h\nu$ to $\alpha=0$.

Figure 3.3. shows the $(\alpha h\nu)^2$ versus $h\nu$ curves of Sn-Cd composite nanorods / nano particles prepared by novel method at 110 ºC temperature.

The dotted lines show the linear fit and corresponding extrapolation. The E_g values for Sn-Cd composite nanorods / nano particles are 2.0 ev Zeng *et al*.

Zeng *et al*., 2008 proposed that the increase in the band gaps of the Sn-Cd composite nanorods / nano particles are indicative of quantum confinement effects, arising owing to their small size. The authers have also attributed the increase in the band gap to quantum confinement effects.

Figure 3.4. and 3.5. shows the absorption versus wavelength and transmittance versus wavelength respectively of the Sn-Cd composite nanorods / nano particles and this due to cluster of nanoparticles and bundles of nano particles. Reflectance of the sample more than 90% than absorption and transmittance and the calculated value of reflectance were tabulated (Table 3.3).

The morphologies of Sn- Cd nano structures were characterized by Scanning

Electron Microscope (SEM). Figure 3.6 – 3.9 shows the detailed morphologies of the Sn – Cd nanorods, nano particles and nano wires. SEM analysis for the sample synthesized under hydrothermal conditions shows the influence of the hydrothermal temperature of the nano structured morphologies. The morphology of the Sn – Cd depends on preparation conditions which the hydrothermal temperature is they further, but reaction is not very important to morphology.

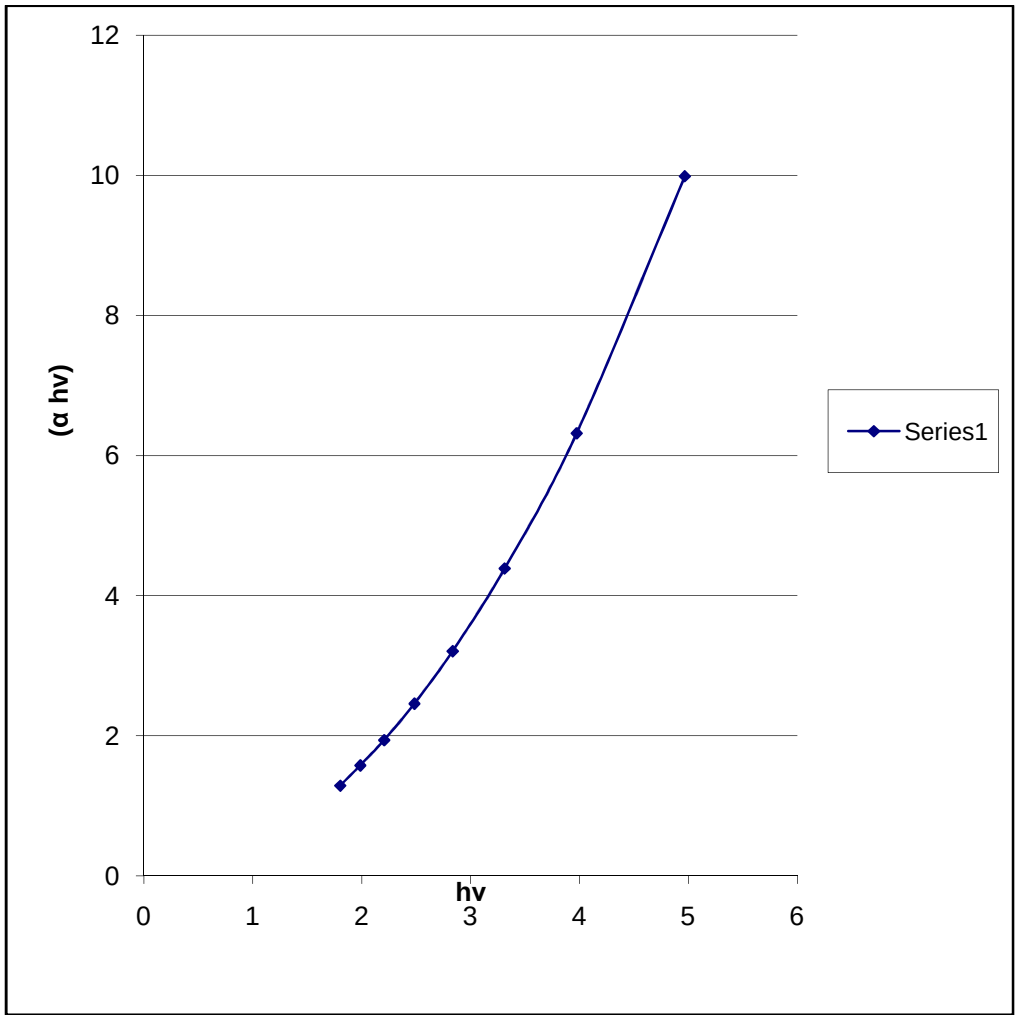

Figure 3.3 Eg diagram of Sn-Cd composite nr,nw & np

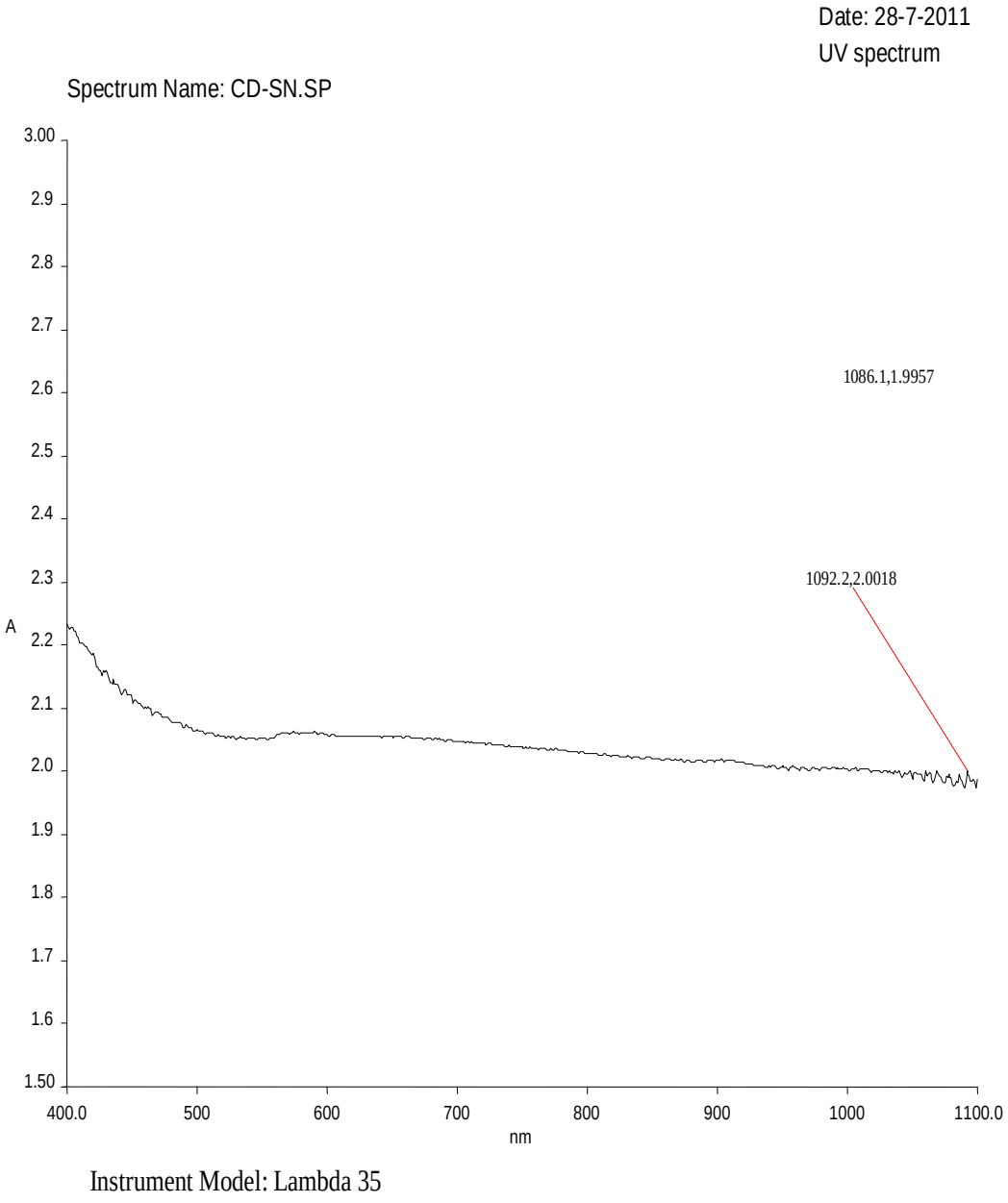

Figure 3.4 UV-Visible Absorption spectrum of Sn-Cd composite nr,nw & np

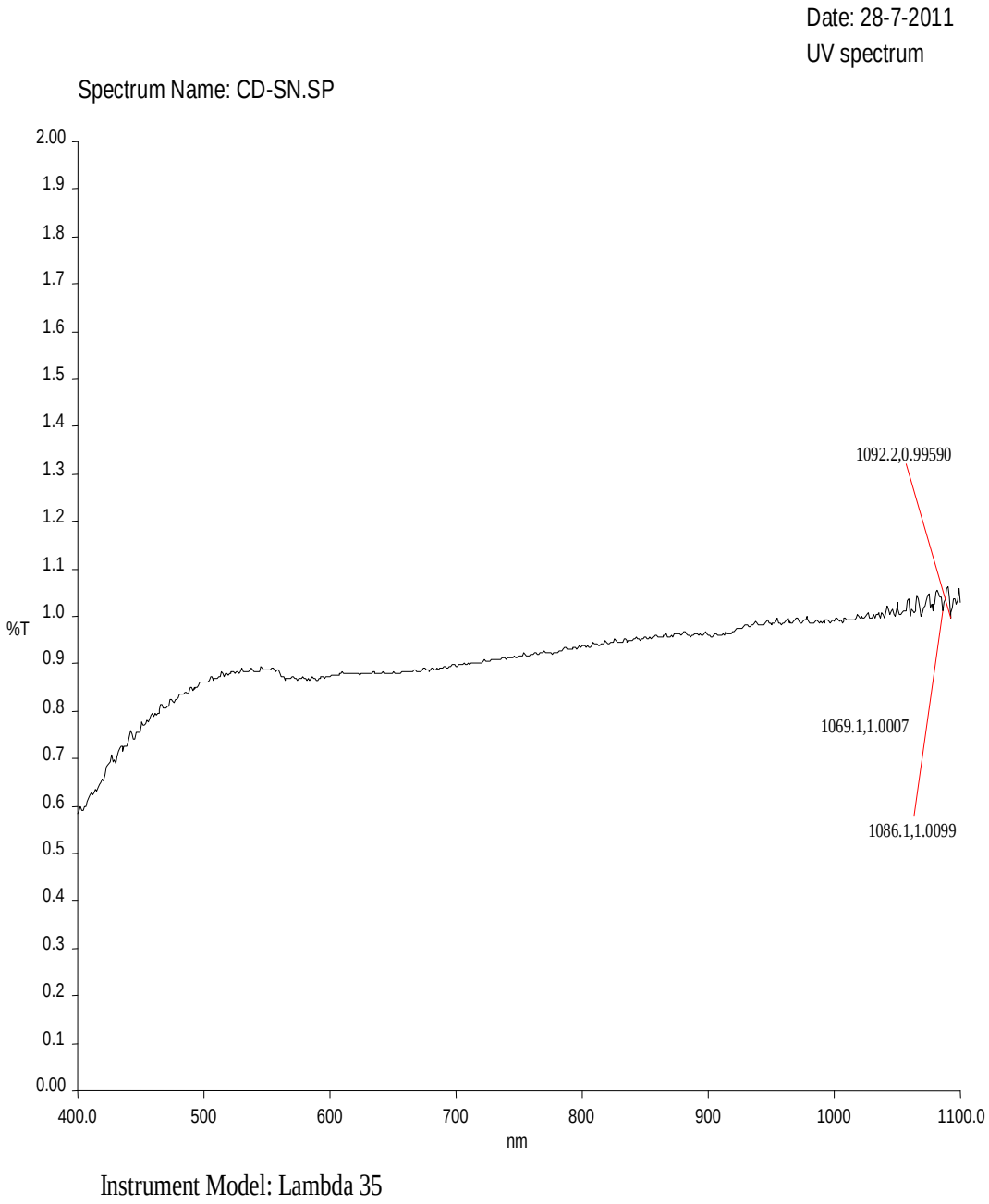

Figure 3.5. Transmission spectrum of Sn-Cd composite nr,nw& np.

Table 3.3. Absorption, Transmission, Reflection Percentage of Sn – Cd Composite nano rods /nano particles

Wavelength In nm	Absorption in %	Transmission in %	Reflection in %
400	2.23	0.59	97.18
500	2.06	0.83	97.11
600	2.07	0.86	97.07
700	2.06	0.88	97.06
800	2.05	0.90	97.05
900	2.01	0.92	97.07
1000	1.98	0.95	97.07
1100	1.97	1.08	96.95

Figure 3.6. shows the cauliflower structure of Sn – Cd nano structures indicates the Tin nano particles on the dip of the Cadmium nano rods / nano wires. The growth direction almost parallel to nr and nws. Using this novel method we have used a good solvent only i.e why structure in micrometer range without stirring. So it is very easy get nano and pico size structure by using magnetic stirrer. Figure also implies that the two growth directions perpendicular to each other. The transmittance of these two elements clearly indicates its properties i.e high transmittance for Sn nano particles and low transmittance of Cd nanorods , nano wires and nano particles comparatively.

Distribution of close view or white tin nano particles sitting over the Cadmium nanorods nano wires and nano particles . Shown in figure 3.7 white and black mixed rods / wires is a Cadmium materials. Also the space between each rods , wires and particles indicates the easy separation during or after synthesis.

Growth direction of Tin nano particles and Cadmium nano rods , wires and particles are very clearly seen in figure 3.8. From the figure it is clear that the cluster of rods / wires and particles in addition to the position of particles on the nano Cadmium rods / wires and rectangular well grown.

Cadmium rods on the rectangular size of the Cadmium rods. Tin particles were placed on the dip of the Cadmium rods are clearly seen in the figure 3.9. If we clearly seen the finishing edge of the Cadmium rods; we found that the fine and curved complete growth nano structures. Further and final close view of Sn-Cd nano structure shows (figure 3.9) that the hexagonal size of Tin nano particles.

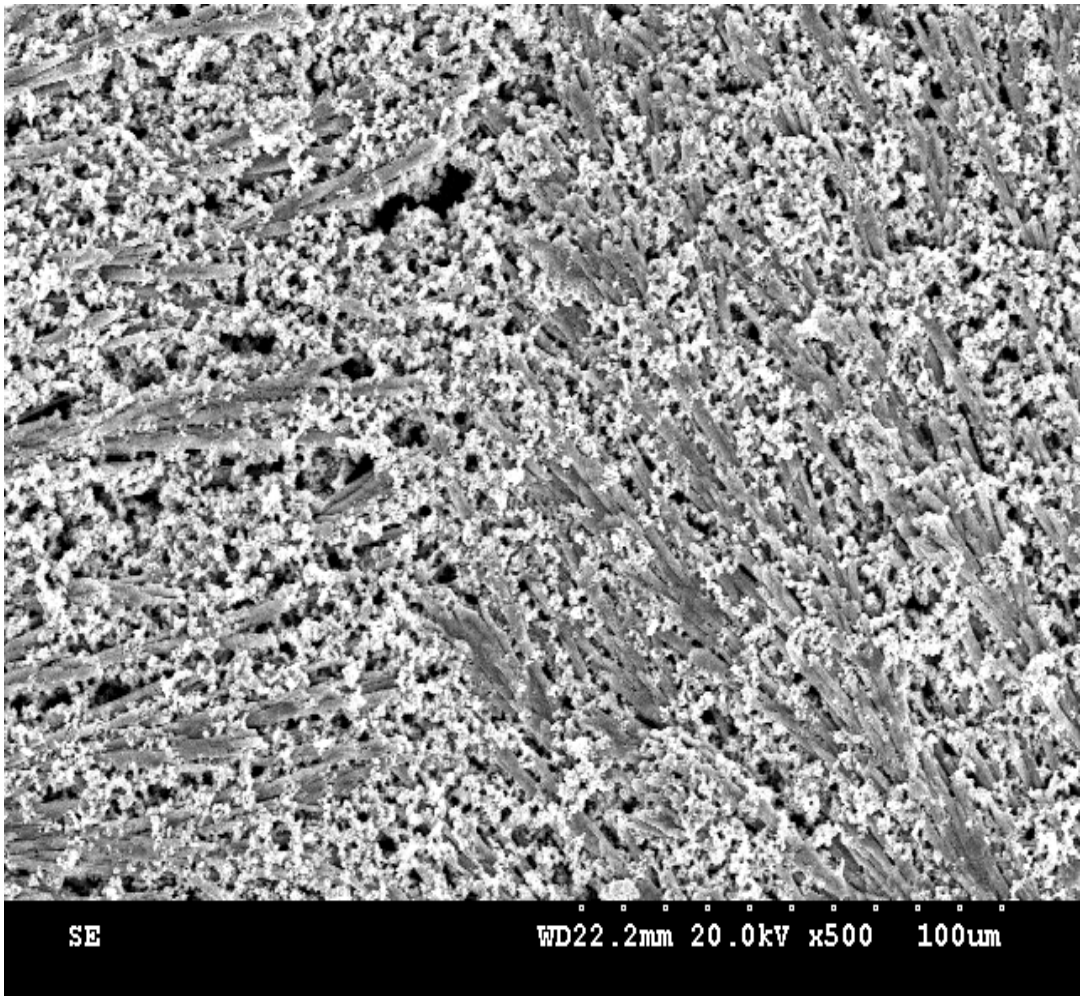

Figure 3.6. SEM Pattern of Sn-Cd composite nano rods/wires and particles at 100µm.

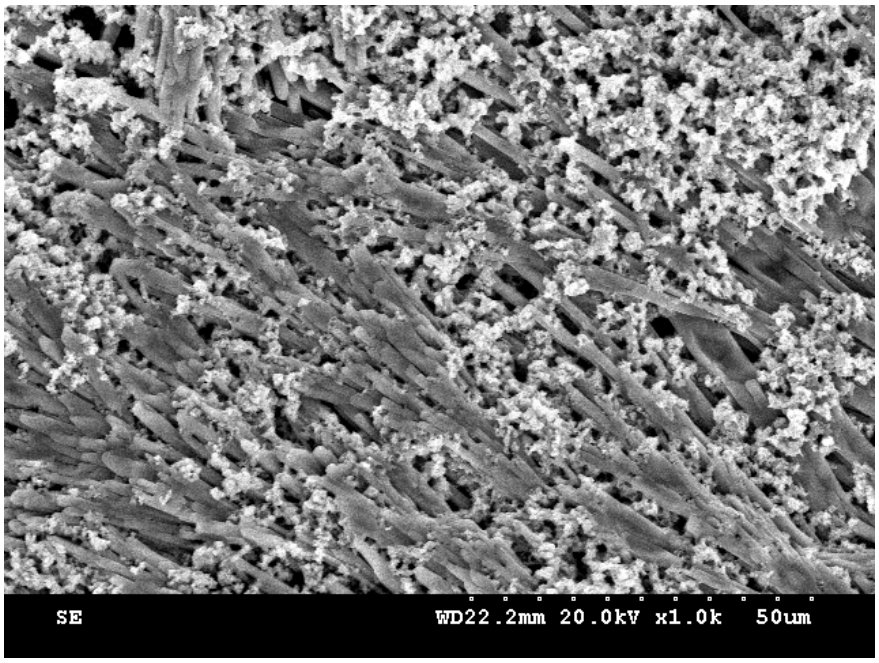

Figure 3.7. SEM image of Sn-Cd composite at 50µm

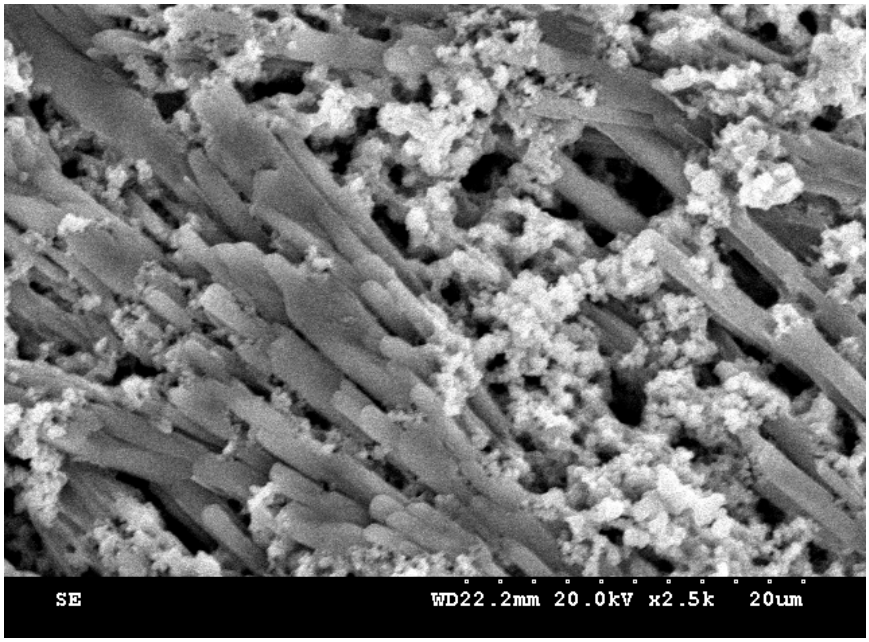

Figure 3.8. Sn-Cd SEM image at 20µm.

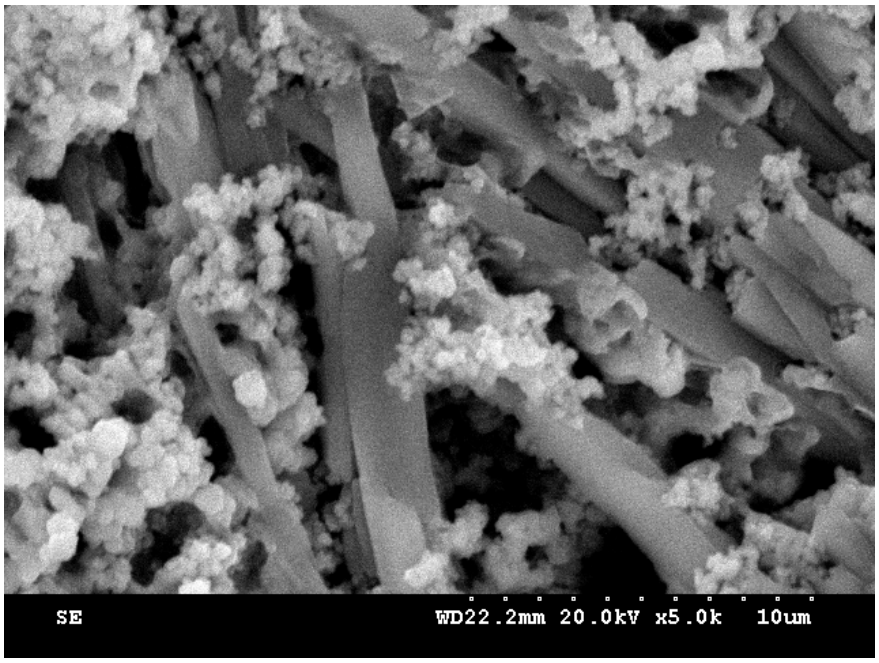

Figure 3.9. Sn-Cd composite nanorods, nanowires and nanoparticls at 10 micrometer

4. CONCLUSION

Sn-Cd nano structures were successfully prepared by novel method under the different hydrothermal treating temperature and time. The samples were analysed by XRD, SEM, UV-Visible spectroscopy.

Sn-Cd composite nanorods / nanowires / nano particles were successfully fabricated by novel method. Using the novel technique it is possible to synthesis nano rods (nr), nano particles (np) and nano wires (nw) simultaneously.

Sn-Cd composite nanorods / nanowires / nano particles were synthesized by the novel method. The new techniques totally different from the existing method. In addition to the preparation of nr, np and nw are the clusters on single glass plate. Growth structure look like cauliflower branched and it was fabricated at 383 K by the applications of the novel techniques.

X – ray diffraction (XRD) peaks indicates the diffraction of x-ray nr, nw and np. Exactly fifty six peaks were found and these are the combination of Sn-Cd nano composites. The average size of the nano rods is 52.69 nm and the rods size ranging from 32.90 nm to 68.70 nm. The d-spacing value of the nanorods varying from 7.6884 Å to 1.2125Å. Dislocation Density values changing from $2.11 – 9.23x10^{14}$ m^{-2}.

Scanning electron microscope (SEM) image of shows Sn-Cd nr, np and nw. The cluster of nr and nps distributed and its top view were presented. Separations of these nano structures were possible using

SEM. The equality of this new method is simultaneously preparation and separation of nr, nw and np at 110^{o}C.

The UV and visible spectrum of Sn-Cd nr, nw and np's where presented and its absorbance and transmittance percentage are 2.23 and 0.059% respectively. The band gap energy value of Sn-Cd nr, nw, np is 2.4 e.V calculated from figure 3.3.

The novel method of Sn-Cd nano structure is a simple and green process that has been receiving under attention recently. Only few morphologies have been reported and research is under way to grow different nano structure through the one of the additives. Sn-Cd nano structure being chemically more stable than binary oxides are attractive candidates for applications in such devices as solar cells, gas and bio-sensors and detectors, to name a few. Sn-Cd nano structures are being increasingly used as photocatalysis.

REFERENCES

1. Agarwal, R.; Barrelet, C. J.; Lieber, C. M. *Nano Lett*., 5, 917. (2005).
2. Andersson, Martin; Österlund, Lars; Ljungström, Sten; Palmqvist, Anders. "Preparation of Nanosize Anatase and Rutile TiO2 by Hydrothermal Treatment of Microemulsions and Their Activity for Photocatalytic
3. Wet Oxidation of Phenol". *The Journal of Physical Chemistry*, (2002).
4. Annamalai.A, Carvalho D, Wilson K. C. and Lee M. *J. Mater. Charact*. 61, 873, (2010).
5. Anukorn Phuruangrat, Titipun Thongtem and Somchai Thongtem; *Journal of Experimental Nanoscience, Vol*.4, No.1, 47–54. (2009).
6. Asit Baran Panda, Garry Glaspell, and M. Samy El-Shall ; *j. Am. Chem. Soc. Vol*. 128, NO. 9, 2791, (2006).
7. Atashbar M Z, Yu M-F and Chen X , Investigation and characterization of Ga2O3 nanowire for gas sensing applications IEEE Sensors. (2002).
8. Barrelet, C. J.; Wu, Y.; Bell, D. C.; Lieber, C. M. *J. Am. Chem. Soc*. 125, 11498, (2003).
9. Bharat Bhushan, Handbook of Nano-technology Part A (Springer) 99 (2004).
10. Friedman, R. S.; McAlpine, M. C.; Ricketts, D. S.; Ham, D.; Lieber, C. M. *Nature*, 434, 1085, (2005).
11. Greytak A B, Lauhon L J, Gudiksen M S and Lieber C M. *Applied Physics Letters* 84 24 (2004).
12. Holleman, Arnold F.; Wiberg, Egon; Wiberg, Nils; "Cadmium" (in German). Lehrbuch der Anorganischen Chemie (91–100 ed.). Walter de Gruyter. pp. 1056–1057. (1985).
13. Hong, B. H.; Bae, S. C.; Lee, C.-W.; Jeong, S.; Kim, K.S., *Science*, 294,348 (2001).
14. Hu, J.; Li, L.; Yang, W.; Manna, L.; Wang, L.; Alivisatos, A. P., *Science*, 292, 2060 (2001).
15. Huang Y, Xiangfeng, Cui Y and Mlieber C, *Nano Letters* 2 (2) 101, (2002).
16. Huynh, W. U.; Dittmer,J. J.; Alivisatos, *A. P. Science*, 295, 2425. (2002).
17. Kan, S.; Mokari, T.; Rothenberg, E.; Banin, *U. Nat. Mater*.2, 155 (2003).
18. Lauhon L J, Gudiksen M S and Lieber C M, Phil. *Trans. R. Soc. Lond*. A 362 1247, (2004).
19. Li,Y; Li,X.; Yang, C.; Li, Y. *J. Phys. Chem. B*, 108, 16002. (2004).

20. Lu, Q.; Gao, F.; Komarneni, S. *J. Mater. Res*., 19, 1649 (2004).
21. Lu, Yicheng; Zhong, Jian, Todd Steiner. ed. Semiconductor Nanostructures for Optoelectronic Applications. Norwood, MA: *Artech House, Inc*.. pp. 191–192. (2004).
22. Liu, X.; Tian, B.; Yu, C.; Tu, B.; Zhao, D. *Chem. Lett*., 33, 522. (2004).
23. Manna, L. Scher, E. C.; Alivisatos, A. P. *J. Am. Chem. Soc*, 122, 12700. (2000).
24. Nedeljkovic, J. M.; Micic, O. I.; Ahrenkil, S. P.; Miedaner, A.; Nozik, A. J. *J. Am. Chem. Soc*, 126, 2632. (2004).
25. Nikoobakht, B.; Wang, Z. L.; El-Sayed, M. A. *J. Phys. Chem. B*, 104, 8635. (2000).
26. Oliveira, Marcela M.; Schnitzler, Danielle C.; Zarbin, Aldo J. G. "(Ti,Sn) O2Mixed Oxides Nanoparticles Obtained by the Sol−Gel Route". *Chemistry of Materials* 15 (9): 1903. (2003).
27. Nikoobakht, B.; Wang, Z. L.; El-Sayed, M. A. *J. Phys. Chem. B*, 104, 8635 (2000).
28. Panda, A. B.; Acharya, S.; Efrima, S. *Adv. Mater*, 17, 2471. (2005).
29. Patently M J Nano materials – the driving force Nanotoday 7 (12) 20, (2004).
30. Peng, X.; Manna, L.; Yang, W.; Wickham, J.; Scher, E.; Kadavanich,
31. A.; Alivisatos. A. P. *Nature*, 404, 59. (2000).
32. Pradhan, N.; Efrima, S. *J. Phys. Chem. B*., 108, 11964 (2004).
33. Quang Trung Khuc, Xuan Hien Vu, Duc Vuong Dang and DucChien Nguyen; *Adv. Nat. Sci.: Nanosci. Nanotechnol*. 1025010 (4pp), (2010).
34. Rahaman, M.N.. Ceramic Processing. Boca Raton: CRC Press. pp. 242–244, (2007).
35. S. Ramanathan, S. Patibandla, S. Bandyopadhyay, J.D. Edwards, J. Anderson, *J. Mater. Sci.: Mater. Electron* 17, 651 (2006).
36. S.sakthivel and D.mangalraj, NANO VISION an International *Journal of Nanoscience and nano technology. Vol*. 1 (1), 47-53, (2011).
37. S.sakthivel and D.mangalraj, NANO VISION an International Journal of Nanoscience and nano technology. Vol.1(1), 15-23, (2011).
38. Tang, Z.; Kotov, N. A.; Giersig, *M. Science*, 297, 237, (2002).
39. Yang P, Wu Y, Fan R, *International Journal of Nanoscience* 1(1) 1, (2002).
40. Yin, M.; Gu,Y.; Kuskovsky, I. L.; Andelman, T.; Zhu, Y.; Neumark, G. F.; O'Brien, S. *J. Am. Chem. Soc*., 126, 6206. (2004).
41. Zeng J, Xin M, Li K, Wang H, Yan H and Zhang W, *J. Phys. Chem, C* 112, 4159, (2008).